The Dynamics of Embolism Repair in Xylem: In Vivo Visualizations Using High-Resolution Computed Tomography[1][C][W][OA]

Craig R. Brodersen, Andrew J. McElrone, Brendan Choat, Mark A. Matthews, and Kenneth A. Shackel*

Department of Viticulture and Enology (C.R.B., A.J.M., M.A.M.) and Department of Plant Sciences (K.A.S.), University of California, Davis, California 95616; United States Department of Agriculture-Agricultural Research Service, Crops Pathology and Genetics Research Unit, Davis, California 95616 (A.J.M.); and Research School of Biology, Australian National University, Canberra, Australian Capital Territory 0200, Australia (B.C.)

Water moves through plants under tension and in a thermodynamically metastable state, leaving the nonliving vessels that transport this water vulnerable to blockage by gas embolisms. Failure to reestablish flow in embolized vessels can lead to systemic loss of hydraulic conductivity and ultimately death. Most plants have developed a mechanism to restore vessel functionality by refilling embolized vessels, but the details of this process in vessel networks under tension have remained unclear for decades. Here we present, to our knowledge, the first in vivo visualization and quantification of the refilling process for any species using high-resolution x-ray computed tomography. Successful vessel refilling in grapevine (*Vitis vinifera*) was dependent on water influx from surrounding living tissue at a rate of 6×10^{-4} μm s^{-1}, with individual droplets expanding over time, filling vessels, and forcing the dissolution of entrapped gas. Both filling and draining processes could be observed in the same vessel, indicating that successful refilling requires hydraulic isolation from tensions that would otherwise prevent embolism repair. Our study demonstrates that despite the presence of tensions in the bulk xylem, plants are able to restore hydraulic conductivity in the xylem.

Vascular plants have evolved a simple but elegant system for long-distance transport of water and minerals through a network of nonliving, pipe-like cells. Whereas long-distance transport in animals is actively driven by positive pressure, most water transport in plants is passively driven by tension as explained by the Cohesion-Tension (C-T) theory (Dixon and Joly, 1894; Tyree, 2003). Water under tension is metastable however (Hayward, 1971), making the transport system inherently vulnerable to cavitation and blockage by gas embolisms (Tyree and Sperry, 1989). Direct measurements of negative pressures (tensions) in xylem (Wei et al., 1999) have confirmed the fundamental basis for the C-T theory of water transport in plants (e.g. Tyree, 2003), but many details regarding the susceptibility of the xylem network to cavitation and blockage by embolisms, and a thermodynamically plausible mechanism for the repair of these embolisms, remain unclear (Clearwater and Goldstein, 2005).

Plants have apparently evolved mechanisms, including root pressure, to remove embolisms and restore water transport in vessels (Sperry et al., 1987; Tibbetts and Ewers, 2000; Isnard and Silk, 2009). Refilling of embolized vessels far from roots (Holbrook et al., 2001) and under a state of tension (Salleo and Gullo, 1986) is not well understood, but most hypotheses involve localized solute export into embolized vessels from adjacent living xylem parenchyma, osmotic movement of water into these vessels, and isolation of the refilling vessel from the tension in its local water environment (Tyree et al., 1999; Hacke and Sperry, 2003; Clearwater and Goldstein, 2005; Salleo et al., 2006). Embolism repair is complicated by the fact that xylem conduits (tracheids and vessels) form an interconnected network. While such a network will provide a low-resistance pathway for the bulk flow of water when the conduits are filled, if a cavitation event and subsequent embolism (gas bubble) either spontaneously occurs within a conduit, or spreads to it from another conduit, the presence of tension in this network should also quickly drain a conduit of its water

[1] This work was supported by the National Science Foundation (grant no. 0818479) and U.S. Department of Agriculture-Agricultural Research Service Current Research Information System funding (research project no. 5306–21220–004–00). The Advanced Light Source is supported by the Director, Office of Science, Office of Basic Energy Sciences, of the U.S. Department of Energy (contract no. DE–AC02–05CH11231).

* Corresponding author; e-mail kashackel@ucdavis.edu.

The author responsible for distribution of materials integral to the findings presented in this article in accordance with the policy described in the Instructions for Authors (www.plantphysiol.org) is: Kenneth A. Shackel (kashackel@ucdavis.edu).

[C] Some figures in this article are displayed in color online but in black and white in the print edition.

[W] The online version of this article contains Web-only data.

[OA] Open Access articles can be viewed online without a subscription.

www.plantphysiol.org/cgi/doi/10.1104/pp.110.162396

and prevent its refilling. The spread of embolisms is limited by the small effective pore size of the connections between conduits (known as pit membranes), but under conditions of low plant water availability, embolisms do occur and spread (Tyree and Zimmermann, 2002; Choat et al., 2008), and evidence for the repair of embolized vessels, despite the presumed presence of a tension throughout the plant xylem, has been obtained in many species (Salleo et al., 1996; McCully et al., 1998; Zwieniecki and Holbrook, 1998; Kaufmann et al., 2009).

A major limitation to the testing of these hypotheses and to our understanding of embolism repair has been the lack of in vivo observations at a sufficient resolution and an appropriate temporal scale to document how the refilling occurs. Here we present a new method for imaging the functional status of vessels using high-resolution x-ray computed tomography (HRCT), providing, to our knowledge, the first in vivo visualization of the refilling process for any species. Previous in vivo measurements of vessel refilling have been performed using NMR imaging, but the resolution was insufficient to determine the source of the refilling water (Holbrook et al., 2001; Scheenen et al., 2007). In vivo imaging at this scale allows for nondestructive visualization and measurement of the change in both air and water volume within the vessel lumen, giving unprecedented access to the mechanisms of embolism repair.

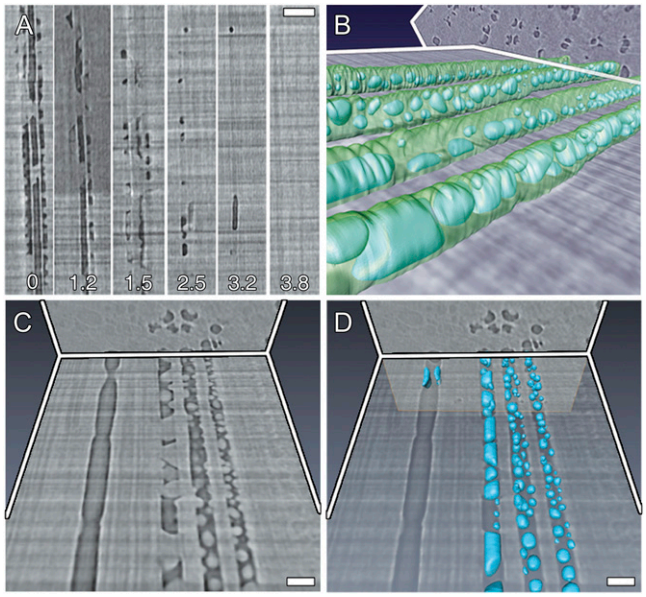

Figure 1. In vivo HRCT sections of a representative grapevine stem undergoing vessel refilling. Time-lapse longitudinal sections (A) showing the refilling of three adjacent vessels and the presence of water droplets on the inner vessel walls (hours indicated in each section). Bar = 200 μm. Trans-longitudinal section with vessel walls and droplets rendered in 3D (B). Trans-longitudinal section showing droplet details in four vessels at different stages of refilling (C), and the corresponding 3D volume rendering (D). Vessel on the far left shows evidence of failed refilling. Bars = 100 μm.

RESULTS

We visualized and quantified the refilling of individual, embolized vessels in grapevine (*Vitis vinifera* 'Chardonnay') plants under a state of tension using in vivo HRCT. Time-lapse analysis of vessels in longitudinal section (Fig. 1A; Supplemental Fig. S1) confirmed that refilling occurred over several hours. Partial liquid filling of vessels was visible in longitudinal (Fig. 1A) and transverse (Supplemental Fig. S2) sections. These two-dimensional (2D) areas of liquid were clearly identified as droplets when sections are integrated into a three-dimensional (3D) volume rendering (Fig. 1, B–D; Supplemental Video S1). The combined images showed that refilling of an individual vessel began with many water droplets forming on the interior vessel walls, followed by coalescence of droplets and compression of the trapped gas embolisms into progressively smaller bubbles until the gas disappeared (Fig. 1A; Supplemental Fig. S1).

The three plants analyzed in this study showed that refilling rates were variable and dependent on water status prior to refilling. Plant A, starting at −0.9 MPa stem water potential (SWP), showed signs of refilling immediately (droplet accumulation and air displacement), and gradually refilled over a 6 h period (Fig. 2A). Irrigation was required to initiate refilling in plants B and C (Fig. 2, B and C), which started at −0.7 and −1.6 MPa SWP, respectively. Plant B was monitored for 2.25 h prior to irrigation with no visible change in the functional status of the vessels, despite starting at a similar SWP as plant A. Thirty minutes after irrigation there was a sharp increase in the number of filled vessels and a gradual increase in the number of refilling vessels, filling approximately 30% of the total vessels in 2 h. Plant B then remained stable for the remainder of the experiment. Plant C showed negligible refilling during the first 3 h of observation. Following irrigation there was a substantial delay (4 h) between the recovery in plant water status and the onset of refilling (Fig. 2C). Plant C then remained stable for approximately 7 h, followed by a rapid increase in refilling.

Within individual vessels, droplets formed nonuniformly around the perimeter of the interior vessel wall (Fig. 3, A and B). The highest frequency occurred in proximity to the ray parenchyma cells, and the lowest frequency ±90° from that point (Fig. 3C). The low droplet frequency at ±90° reflects the low frequency of living parenchyma cells at those angles (Supplemental Fig. S3), because vessel-vessel connections are most often aligned radially and parallel to the rays, thereby displacing parenchyma cells in those positions.

Droplets visualized with HRCT generally resembled those observed with cryo-scanning electron microscopy (SEM) in other species (Canny, 1997; Utsumi

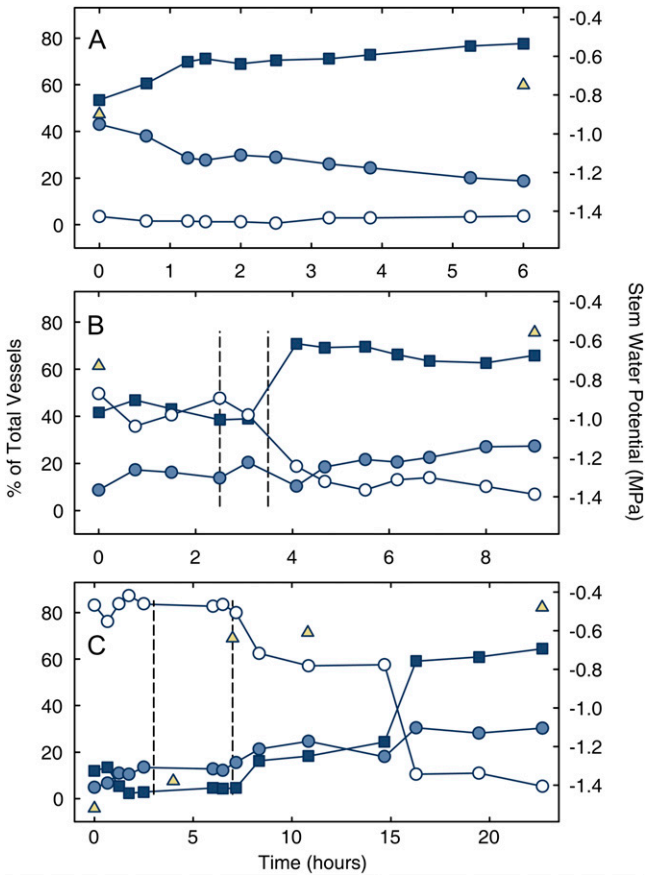

Figure 2. Change in the refilling status of grapevine vessels. Three separate experiments (A–C) showing an increase % filled vessels (squares) and a decrease in % empty (shaded circles) and filling (white circles) vessels over time (note difference in *x* axis scales). SWP increased over time (triangles), n = 593, 480, and 394 total vessels for experiments A to C, respectively. Vertical dashed lines in B and C mark supplemental water additions. [See online article for color version of this figure.]

et al., 1998; Canny et al., 2007). However, some droplets exhibited variable contact angles to the wall around their perimeter (Fig. 1, A–C; Supplemental Fig. S2), indicating both hydrophobic and hydrophilic wall surfaces in close proximity. The average droplet contact angle to the wall was variable (94° ± 27 SD for 100 droplets, representing three plants) and independent of droplet size. As droplets increased in volume, they spread along the wall until reaching a hydrophobic area, and continued to expand without further spreading along the wall. Droplets emerging from opposite sides of vessels spanned the vessel lumen, forming water columns with low contact angles (40.5° ± 16.7 SD for 100 air water interface areas), and creating pockets of gas.

Tracking the functional status of vessels over time provided in vivo documentation of droplet growth in plants, and revealed both successes and failures in embolism repair (Fig. 4, A and C). The average volume increase for 19 individual droplets from seven vessels was 6.0 $\mu m^3\ s^{-1}$ $droplet^{-1}$. Twelve of these droplets were observable and measured as discrete individuals for three or four points in time (75–90 total minutes), and volume growth over time was essentially linear (R^2 = 0.84 − 1.00, mean = 0.92; Supplemental Fig. S4), with significant differences in individual droplet growth rate within vessels (Supplemental Table S1). Droplet density was approximately 100 droplets mm^{-2} of inside vessel surface, averaged from 25 vessels of different diameter from all three experimental plants (Supplemental Fig. S5). Droplet formation was not biased toward the top or bottom of the scanned stem area.

To test whether overall refilling rates could be attributed to the combined effect of the number of droplets and their growth rates, we compared empirically measured changes in water volume to predicted volume changes for 11 independent vessels (data for some vessels shown in Fig. 4A). The predicted calculations were based on the vessel-specific wall area, average droplet density, and an average droplet growth rate, and we found very good agreement to the observed change (Fig. 4B; Supplemental Fig. S4; Supplemental Table S1).

Gas bubbles were observed in two possible states: (1) suspended in the vessel, surrounded completely by water, or (2) in contact with the vessel wall (Fig. 1A; Supplemental Fig. S1). Bubbles surrounded by water were verified by panning through longitudinal and transverse HRCT images and confirming that water was clearly visible between the bubble and vessel wall on all sides. Bubbles surrounded by water eventually collapsed between measurements (approximately 30 min, Fig. 1A; Supplemental Fig. S1), consistent with the proposed kinetics of gas dissolution directly into solution (Epstein and Plesset, 1950; Shen et al., 2003; Hölttä et al., 2007).

DISCUSSION

The visualization and analysis of embolism repair presented in this study illustrates the utility of HRCT as an in vivo imaging tool. This method provides unprecedented access to live plant tissue at a spatial and temporal resolution that facilitates the study of the functional status of vessels over time. Unlike NMR imaging, cryo-SEM, acoustic emissions, and other methods used to measure embolism spread and repair, HRCT provides quantitative data for individual vessels paired with a 3D visualization of refilling mechanism.

Ray parenchyma have been suggested as a potential pathway for solute transport from the phloem to vessels (Salleo et al., 1996; Tyree et al., 1999; Salleo et al., 2006), and the droplet distribution we observed is consistent with a radial translocation of solutes from rays to the xylem parenchyma that have pit connections to embolized vessels. Nonliving fibers and living ray and paratracheal parenchyma surround grape-

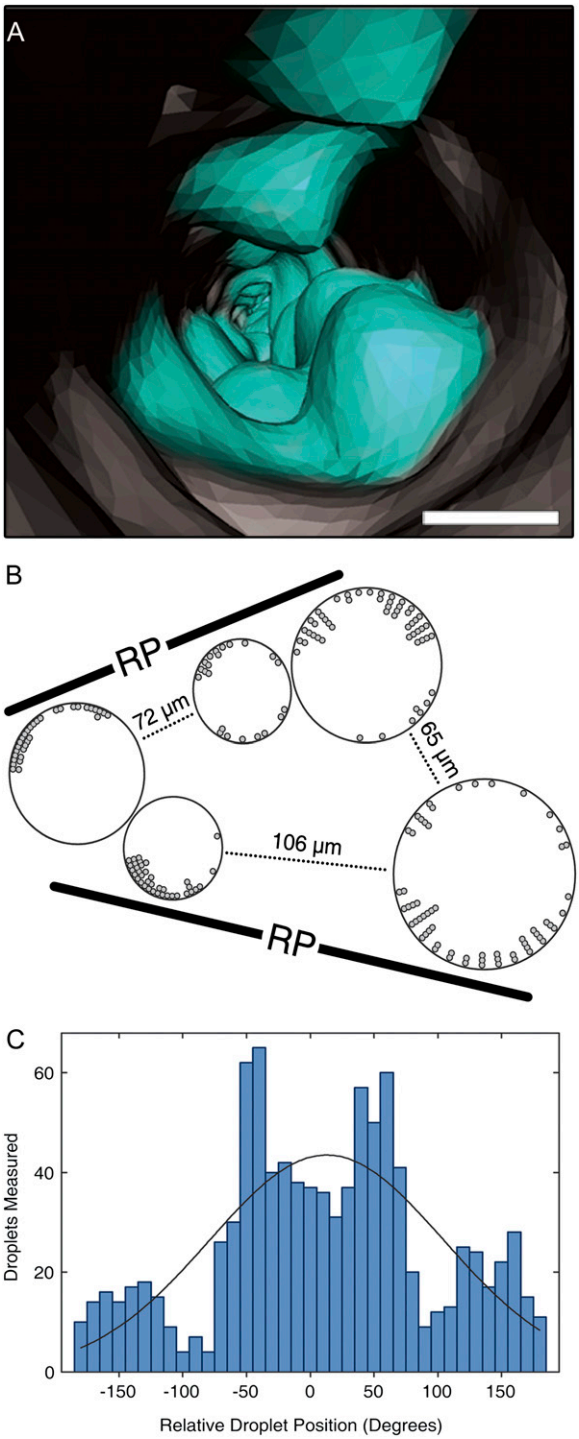

Figure 3. Droplet distribution in refilling vessels. Volume rendering of the inside of a filling vessel (A) with water droplets (blue), many aligned vertically on opposite sides of the vessel. Bar = 30 μm. Example map of five vessels (B), dark symbols represent droplet entry points around the vessel wall perimeter (one symbol = three drops). Black bars represent the orientation of the ray parenchyma cells (RP). Combined histogram (C) for the number of droplets observed around the inner circumference of 22 vessels from three plants (n = 976 droplets) as a function of the position relative to the point closest to the ray parenchyma cells (relative position = 0°), showing the highest frequencies near ±45° and lowest frequencies near ±90°. Black line = normal distribution with the same mean and SD as the observed distribution, although the observed distribution was clearly nonnormal ($P < 0.001$). [See online article for color version of this figure.]

vine vessels in a pattern that implicate their role in the refilling mechanism visualized here (Supplemental Fig. S3). Grapevine vessels are known to cavitate (Tyree and Sperry, 1989) and subsequently fill with tyloses and/or gels (Sun et al., 2008) that prevent the systemic spread of embolism. The anatomical similarity among tylose, gel, and now droplet formation (Fig. 2B) indicates that living paratracheal parenchyma cells perform multiple roles in regulating water transport in plants through both maintenance and termination of vessel functionality, further illustrating the importance of living processes in water transport through the xylem (Zwieniecki et al., 2001a).

Droplet growth and vapor volume measurements indicate that the kinetics of vessel refilling can be attributed to growth and coalescence of droplets. Based on these data, we estimate an overall average refilling flux (water volume per unit area of vessel wall per unit time) of 6×10^{-4} μm s^{-1}, although a wide range was observed in both droplet density (Supplemental Fig. S5) and droplet growth rate (Supplemental Fig. S4), giving a 2 orders of magnitude range (10^{-5}–10^{-3} μm s^{-1}) for this estimate. Using the average rate, about 2.3 h would be required to fill the circular area of the empty lumen area of a 20 μm diameter vessel, and 17.3 h for a 150 μm diameter vessel. To our knowledge, these are the first direct observations of vessel refilling in plants under tension, but mathematical modeling (Vesala et al., 2003) and NMR imaging of refilling in roots (Kaufmann et al., 2009) both estimate refilling times on the order of hours. The only other direct estimate of vessel refilling flux is 7×10^{-2} micron s^{-1} in *Cucumis sativus* (Scheenen et al., 2007) that is above our upper estimate, but for a contrasting species of plant. An alternative approach for estimating a refilling rate has been to calculate a minimum flux needed to balance the expected rate of drainage from a vessel to its surroundings. Using a previously reported vessel radial hydraulic permeability of 2.26×10^{-7} m MPa^{-1} s^{-1} in *Fraxinus americana* (Zwieniecki et al., 2001b), and an assumed local tension of −0.7 MPa (our observations), we calculate that a minimum flux would be 0.16 μm s^{-1}, or about 3 orders of magnitude larger than our estimate. Differences in vessel diameters and species-specific vessel wall and membrane properties between *Fraxinus* and *Vitis* may account for this discrepancy. A higher rate of water loss to the surrounding tissue also implies the net rates we observed were much less than the true gross rate. An alternative hypothesis would be that refilling can be attributed to the observed rates of droplet growth (Fig. 4B) and water loss to the surrounding tissue is less than suggested by Zwieniecki et al. (2001b) if the radial hydraulic permeability is substantially less than the current estimate, or if the

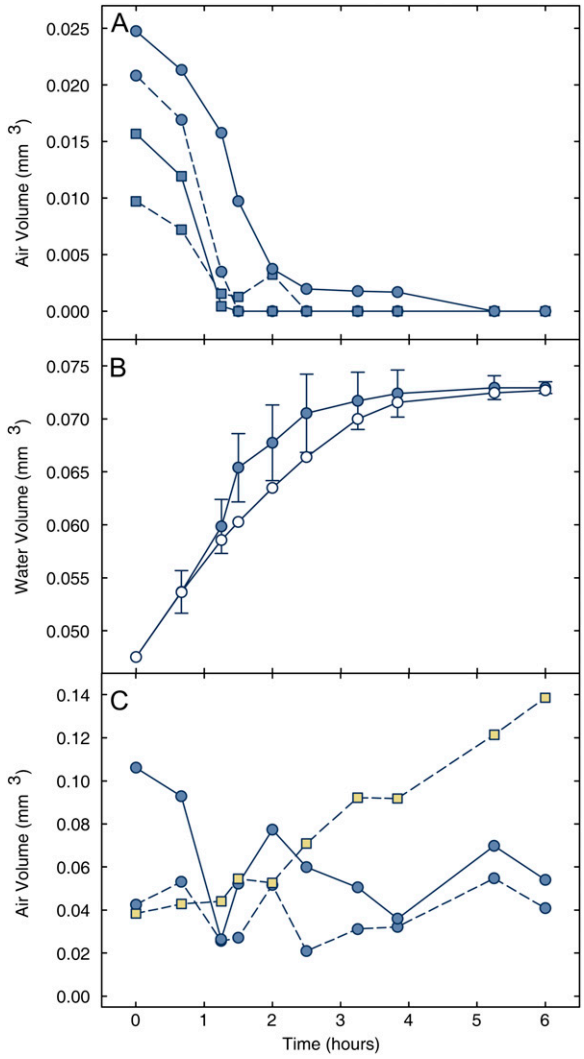

Figure 4. Change in the refilling status of grapevine vessels. Air volume change in the lumen of representative vessels exhibiting successful refilling (A). Average volume of lumen occupied by liquid water (B) observed during successful vessel refilling (shaded symbols, ±2 SE, n = 11) and the predicted volume (white symbols) based on an average droplet growth rate and droplet density from an independent sample of vessels. Air volume change in vessels exhibiting refilling failures (C). Square symbols represent the air volume change of the vessel in Figure 4. [See online article for color version of this figure.]

refilling activity that we observed in initially empty or partially filled vessels is also occurring in neighboring vessels that are full.

Grapevines typically experience a range in SWP over the day and as a result of soil water deficits, and the values measured in these experiments fall within a range not uncommon in the field (Schultz and Matthews, 1988; Choné et al., 2001). Recent experiments have shown 5% to 20% loss of hydraulic conductivity in grapevine at the lowest SWP measured in this study (−1.6 MPa; Choat et al., 2008). Thus, grapevines experiencing moderate drought stress conditions (around −1.2 MPa) have embolized vessels that can be refilled by the plant. Due to the length of time required to repair embolisms in larger diameter vessels, some plants may not fully recover by the time transpiration resumes the following day. Both Hacke and Sperry (2003) and Holbrook et al. (2001) observed a delay in refilling after recovery in SWP, similar to the delays reported here. However, Holbrook et al. (2001) additionally found that refilling only occurred after illumination was ceased. Refilling delays may be the result of water deficit impeding the generation or transduction of the yet unknown signals that trigger refilling. Our data suggest a complex series of events that allow plants to respond to drought-induced embolism that is dependent on plant water status prior to and during refilling.

The fate of the gas phase in refilling vessels is of particular concern (Zwieniecki and Holbrook, 2009), and prior to complete refilling vapor bubbles were visible in two states, either surrounded by water or adhering to the vessel wall. Surface texture and other wall properties influence gas bubble formation in vessels (Kohonen and Helland, 2009), and a high wettability is believed to facilitate the refilling process by surrounding embolisms with water (Kohonen, 2006; Konrad and Roth-Nebelsick, 2009), thereby increasing the surface area available for gas dissolution. Stable bubble-to-wall contact positions over time indicate the presence of hydrophobic portions of the wall, consistent with the hypothesis that gas escapes through hydrophobic gas-filled channels (Zwieniecki and Holbrook, 2009). Hence, our observations provide support for both models of gas removal in grapevine (escape through hydrophobic channels and direct dissolution), but variability in vessel surfaces could allow for alternate mechanisms in other species.

Possible Mechanisms for the Prevention of Refilling Failure

An individual refilling vessel is at risk of being drained by adjacent vessels that are under tension if the refilling vessel is not hydraulically isolated from its surroundings (Vesala et al., 2003; Clearwater and Goldstein, 2005). Refilling occurred at tensions of −0.6 to −0.8 MPa in our experiments (Fig. 5; Supplemental Fig. S6), and indeed, some partially filled vessels failed to refill (i.e. a net loss of water despite the transient presence of water droplets; Figs. 4C and 5; Supplemental Figs. S6 and S7). Vessels exhibiting refilling failures typically shared a wall with an adjacent vessel that was water filled, and hence presumably under tension, at the start of the experiment. The vessel shown in Figure 5 progressively emptied of water over time (Fig. 4C, squares, dashed line), despite simultaneous refilling activity in the same vessel (droplet at white arrow in Fig. 5, time = 0; Supplemental Fig. S7), and successful refilling in a nearby vessel group (Fig. 5). Individual droplets in this vessel eventually disappeared, presumably becoming part of a surface film on the interior vessel wall.

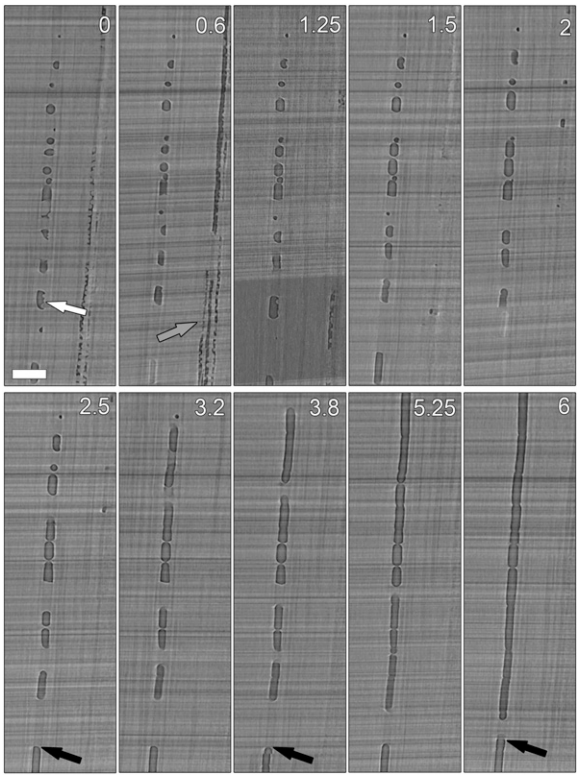

Figure 5. Representative refilling failure in a vessel sharing walls with filled vessels under tension. White arrow indicates identifiable water droplets (see Supplemental Fig. S7 for detail). Black arrows show a stable position of water loss over time, presumably pulled into neighboring vessels under tension. Gray arrow shows concurrent successful refilling in nearby vessels. Numbers = hours. Bar = 350 μm.

Plants may have evolved a mechanism to combat refilling failures by coordinating refilling efforts in adjacent vessels and by maintaining solute transport even after refilling is complete. Refilling was often observed within the same time frame for closely grouped, small diameter vessels. Coordinated solute transport into neighboring vessels during and after filling may delay the occurrence of tension in filled vessels as the group reconnects to the transpiration stream, allowing all members of the group to successfully refill and come under tension gradually rather than suddenly. Coordination may be based on the stimulus that initiates refilling, and both cavitation-induced vibrations and plant hormones have been suggested (Bucci et al., 2003; Scheenen et al., 2007; Salleo et al., 2008). Both of these signals are diffuse and would be expected to initiate refilling activity in vessel groups rather than a single target vessel. The nonselective nature of these signals may be responsible for the widespread refilling that we observed. These data also give support to a localized solute accumulation signal, as proposed by Zwieniecki and Holbrook (2009), because refilling in our experiments was observed in nontranspiring plants.

Prior to this study, cryo-SEM techniques (Canny, 1997; Utsumi et al., 1998; Canny et al., 2007) produced the most compelling evidence for the formation of water droplets on vessel walls during the refilling process, although it has not been clear if these droplets represent artifacts of the freezing process (Cochard et al., 2000; Richter, 2001). The benefits of HRCT include nondestructive, 3D visualizations that can be made on a short time scale (approximately 30 min). Viewing droplet formation and growth from any angle provides an unprecedented visualization of the refilling process without the potential artifacts that may be associated with cryopreservation.

CONCLUSION

These data provide unequivocal evidence of vessel refilling from cells surrounding the xylem. Rather than filling from the bottom up, as might be expected from root pressure, which is well known to occur in grapevines (Isnard and Silk, 2009), droplets entered from many entry points oriented from the rays, as predicted by a refilling mechanism driven by solute pumping into vessels via pits from adjacent parenchyma (Hacke and Sperry, 2003; Salleo et al., 2006, 2009). Here we present an integrated model for vessel refilling (Fig. 6) that incorporates the phloem-loading and solute-

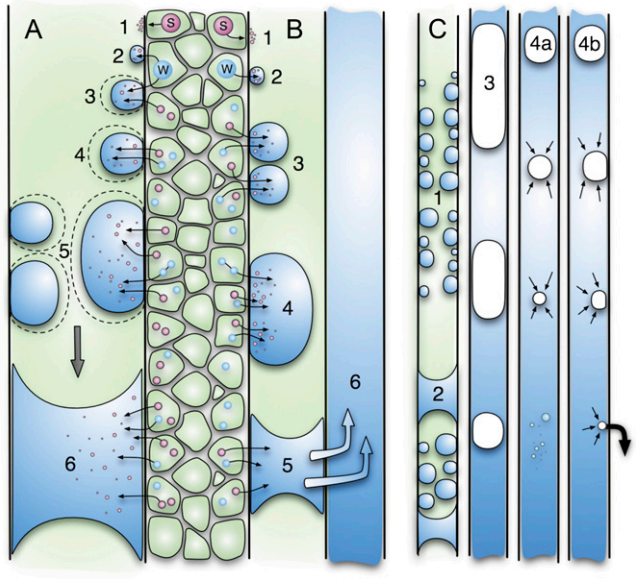

Figure 6. Embolism repair model for grapevine. Embolisms trigger surrounding cells to secrete solutes (S) into the vessel, establishing an osmotic gradient drawing water (W) from the surrounding fibers and parenchyma cells into the vessel (A, 1–2). Water droplets grow until they coalesce, spanning the width of the vessel (A, 3–6). If the refilling vessel is in direct contact with another filled vessel under tension then the water may drain to the neighbor, causing the vessel to empty (B, 1–6). Vessels that receive sufficient water to overcome loss to a neighbor successfully refill (C, 1–3), compressing the remaining gas until it dissolves into solution (C, 4a) or escapes into surrounding hydrophobic microchannels in the vessel wall (C, 4b).

driven refilling mechanisms already proposed (Sauter et al., 1996; Holbrook and Zwieniecki, 1999; Tyree et al., 1999; Hacke and Sperry, 2003; Améglio et al., 2004; Salleo et al., 2006; Zwieniecki and Holbrook, 2009), with an amendment that allows for successful and unsuccessful refilling, and two possible fates for vapor trapped within vessels.

Due to the presence of wetted walls and bubbles surrounded by water late in the refilling process, hydraulic isolation by nonwetted pit areas (pit valve hypothesis; Holbrook and Zwieniecki, 1999; Hacke and Sperry, 2003) does not appear to be possible in grapevine, particularly in light of our observation of droplets appearing in vessels that are simultaneously draining to neighboring vessels (Fig. 4; Supplemental Fig. S7). It is a reasonable assumption that the majority of water transport in plants occurs as proposed over 100 years ago in the C-T theory (Dixon and Joly, 1894), but under some conditions water transport can be considered as assisted by the refilling process described here, and as previously suggested (Canny, 1995; Zimmermann et al., 2004), plant water transport may no longer be regarded as an entirely passive process. Embolism repair is a dynamic process that operates under conditions of local variability in water, solute, and pressure gradients, and in conduit surface wettability. These data illustrate that plants have remarkable control over the flow and distribution of water, and use this control to reverse vessel blockages by embolisms.

MATERIALS AND METHODS

HRCT

Grapevines (*Vitis vinifera* 'Chardonnay') were grown in a greenhouse from cuttings in 10 × 10 × 10 cm pots to a height of approximately 50 cm. Irrigation was removed three to 5 d prior to the beginning of each experiment to induce cavitation of vessels. Plants were transported by car from the University of California, Davis to the x-ray microtomography facility at the Advanced Light Source, Berkeley, California (Beamline 8.3.2). Prior to HRCT scanning, leaves were bagged for 30 min and SWP was measured using a Scholander pressure chamber. Leaves were removed periodically between scans to monitor SWP. During the second and third experiments each plant received two 60 mL doses of deionized water approximately 1 h apart.

The plants were placed in a custom-built aluminum cage and mounted on an air-bearing stage. The leaves and stem were covered in plastic wrap and inserted into a 10 cm diameter Plexiglass cylinder to reduce vibrations, stem movement, and prevent transpiration during the scans. The plant was rotated in the 15 keV synchrotron x-ray beam from 0 to 180 degrees in increments of 0.25 degrees yielding 720, 2D projections per sample. For each plant, a 5 mm section of internode stem tissue approximately 3 cm above the soil surface was repeatedly scanned at a 4.4 μm resolution every 30 to 120 min. Each projection was magnified through a series of lenses and relayed onto a 4,008 × 2,672 pixel CCD camera (#PCO 4000, Cooke Corporation). Raw 2D tomographic projections were reconstructed into approximately 850 sample TIF image slices using Octopus 8.3 software (Institute for Nuclear Sciences). These images were analyzed in Avizo 6.1.1 software (VSG, Inc.), where vessel refilling, droplet growth, air volumes, and droplet distribution data could be analyzed.

HRCT Image Analysis

Images were viewed and analyzed using Avizo 6.1.1 software. Vessel diameters, length, droplet size, air volume, and water volume were measured using the Avizo software that calculated distances and volumes based on the x, y, and z coordinates of individual voxels. Water and air volumes were calculated by segmenting the two materials based on their relative mass attenuation coefficients that are translated into an intensity value for each voxel. Vessel and water droplet volume renderings were created using Avizo software based on these same intensity values and voxel volume of 4.4 μm^3. Twenty-eight vessels from three plants were given a unique identity, and the change in air volume inside these vessels was calculated for each scan in the time series. Droplets on the vessel walls were also identified and their volume change was measured over time. Vessel refilling was measured by categorizing vessels into three different states: air filled, water filled, and an intermediate state where vessels were filled with both water and air. The functional state of each vessel was determined by viewing the vessel lumen using longitudinal and transverse HRCT sections at each time point. The total number of vessels was measured by taking a transverse cross section through the scanned stem area using a sliding microtome. The stem section was mounted on a slide and imaged at 2.5× magnifications using a dissecting microscope and a Nikon D40 digital SLR camera (Nikon Inc.). Higher magnification images were acquired with an Olympus Vanox light microscope (Olympus America, Inc.) at 10× and 20× magnification and imaged using a Pixis CCD digital camera (Princeton Instruments).

The relative position of the water droplets entering vessels was determined by viewing serial transverse HRCT sections longitudinally through the plant stem. Droplets were located on the vessel wall and using the 3D angle tool in Avizo, one line was drawn parallel to the ray parenchyma cells through the middle of the vessel, and a second line was drawn from the origin of the droplet on the vessel wall to the center of the vessel. The angle formed between these two lines was used to determine the point of origin of the vessel droplet with respect to the ray parenchyma cells. Directionality data from 20 vessels, representing three plants, were analyzed using a normality test in SAS (SAS Institute Inc.). Directionality data were plotted using Sigmaplot 11.0 (Systat Software Inc.). All other calculations and statistical analyses were performed in SAS.

Supplemental Data

The following materials are available in the online version of this article.

Supplemental Figure S1. Longitudinal HRCT refilling time series showing the compression and dissolution of gas bubbles in the xylem.

Supplemental Figure S2. In vivo refilling of grapevine vessels.

Supplemental Figure S3. Distribution of cell types surrounding xylem vessels in grapevine.

Supplemental Figure S4. Volume change of 12 individual droplets visualized with time-lapse HRCT scans.

Supplemental Figure S5. Relationship between the total number of drops in a vessel and the internal surface area.

Supplemental Figure S6. Longitudinal HRCT time series showing refilling failure.

Supplemental Figure S7. Magnified HRCT scan from Figure 5A.

Supplemental Table S1. ANOVA data describing the observed and predicted results from droplet growth and refilling analysis.

Supplemental Video S1. 3D reconstruction of refilling vessels in grapevine.

ACKNOWLEDGMENTS

The authors thank A. MacDowell of beamline 8.3.2 at the Lawrence Berkeley National Laboratory Advanced Light Source for technical assistance, A. Walker for grapevine allocation services, and C. Manuck and K. Zhao for data collection and analysis.

Received July 6, 2010; accepted September 8, 2010; published September 14, 2010.

LITERATURE CITED

Améglio T, Decourteix M, Alves G, Valentin V, Sakr S, Julien JL, Petel G, Guilliot A, Lacointe A (2004) Temperature effects on xylem sap osmo-

larity in walnut trees: evidence for a vitalistic model of winter embolism repair. Tree Physiol **24:** 785–793

Bucci S, Scholz F, Goldstein G, Meinzer F, Sternberg L (2003) Dynamic changes in hydraulic conductivity in petioles of two savanna tree species: factors and mechanisms contributing to the refilling of embolized vessels. Plant Cell Environ **26:** 1633–1645

Canny M (1995) A new theory for the ascent of sap-cohesion supported by tissue pressure. Ann Bot (Lond) **75:** 343–357

Canny M (1997) Vessel contents during transpiration-embolisms and refilling. Am J Bot **84:** 1223

Canny M, Sparks J, Huang C, Roderick M (2007) Air embolisms exsolving in the transpiration water—the effect of constrictions in the xylem pipes. Funct Plant Biol **34:** 95–111

Choat B, Cobb AR, Jansen S (2008) Structure and function of bordered pits: new discoveries and impacts on whole-plant hydraulic function. New Phytol **177:** 608–625

Choné X, Van Leeuwen C, Dubourdieu D, Gaudillere J (2001) Stem water potential is a sensitive indicator of grapevine water status. Ann Bot (Lond) **87:** 477–483

Clearwater M, Goldstein G (2005) Embolism repair and long distance water transport. *In* N Holbrook, M Zwieniecki, eds, Vascular Transport in Plants. Elsevier Academic Press, Burlington, MA, pp 375–399

Cochard H, Bodet C, Améglio T, Cruiziat P (2000) Cryo-scanning electron microscopy observations of vessel content during transpiration in walnut petioles: facts or artifacts? Plant Physiol **124:** 1191–1202

Dixon H, Joly J (1894) On the ascent of sap. Ann Bot (Lond) **8:** 468–470

Epstein P, Plesset M (1950) On the stability of gas bubbles in liquid gas solutions. J Chem Phys **18:** 1505–1509

Hacke U, Sperry J (2003) Limits to xylem refilling under negative pressure in *Laurus nobilis* and *Acer negundo*. Plant Cell Environ **26:** 303–311

Hayward A (1971) Negative pressure in liquids; can it be harnessed to serve man? Am Sci **59:** 434–443

Holbrook NM, Ahrens ET, Burns MJ, Zwieniecki MA (2001) In vivo observation of cavitation and embolism repair using magnetic resonance imaging. Plant Physiol **126:** 27–31

Holbrook NM, Zwieniecki MA (1999) Embolism repair and xylem tension: do we need a miracle? Plant Physiol **120:** 7–10

Hölttä T, Vesala T, Nikinmaa E (2007) A model of bubble growth leading to xylem conduit embolism. J Theor Biol **249:** 111–123

Isnard S, Silk W (2009) Moving with climbing plants from Charles Darwin's time into the 21st century. Am J Bot **96:** 1205–1221

Kaufmann I, Schulze-Till T, Schneider HU, Zimmermann U, Jakob P, Wegner LH (2009) Functional repair of embolized vessels in maize roots after temporal drought stress, as demonstrated by magnetic resonance imaging. New Phytol **184:** 245–256

Kohonen M, Helland Å (2009) On the function of wall sculpturing in xylem conduits. J Bionics Eng **6:** 324–329

Kohonen MM (2006) Engineered wettability in tree capillaries. Langmuir **22:** 3148–3153

Konrad W, Roth-Nebelsick A (2009) The influence of the wall contact angle on gas bubble behaviour in xylem conduits under tension and possible consequences for embolism. *In* B Thibaut, ed, Proceedings of the Sixth Plant Biomechanics Conference. Institut für Angewandte Physik, Vienna, pp 32–39

McCully M, Huang C, Ling L (1998) Daily embolism and refilling of xylem vessels in the roots of field-grown maize. New Phytol **138:** 327–342

Richter H (2001) The cohesion theory debate continues: the pitfalls of cryobiology. Trends Plant Sci **6:** 456–457

Salleo S, Gullo M (1986) Xylem cavitation in nodes and internodes of whole *Chorisia insignis* HB et K. plants subjected to water stress: relations between xylem conduit size and cavitation. Ann Bot (Lond) **58:** 431–441

Salleo S, Lo Gullo M, de Paoli D, Zippo M (1996) Xylem recovery from cavitation-induced embolism in young plants of *Laurus nobilis*: a possible mechanism. New Phytol **132:** 47–56

Salleo S, Trifilò P, Esposito S, Nardini A, Lo Gullo M (2009) Starch-to-sugar conversion in wood parenchyma of field-growing *Laurus nobilis* plants: a component of the signal pathway for embolism repair? Funct Plant Biol **36:** 815–825

Salleo S, Trifilo P, Lo Gullo M (2006) Phloem as a possible major determinant of rapid cavitation reversal in stems of Laurus nobilis(laurel). Funct Plant Biol **33:** 1063–1074

Salleo S, Trifilò P, Lo Gullo M (2008) Vessel wall vibrations: trigger for embolism repair. Funct Plant Biol **35:** 289–297

Sauter J, Wisniewski M, Witt W (1996) Interrelationships between ultrastructure, sugar levels, and frost hardiness of ray parenchyma cells during frost acclimation and deacclimation in poplar (*Populus* x *canadensis* Moench 'robusta') wood. J Plant Physiol **149:** 451–461

Scheenen TW, Vergeldt FJ, Heemskerk AM, Van As H (2007) Intact plant magnetic resonance imaging to study dynamics in long-distance sap flow and flow-conducting surface area. Plant Physiol **144:** 1157–1165

Schultz HR, Matthews MA (1988) Resistance to water transport in shoots of *Vitis vinifera* L.: relation to growth at low water potential. Plant Physiol **88:** 718–724

Shen F, Wenji L, Rongfu G, Hu H (2003) A careful physical analysis of gas bubble dynamics in xylem. J Theor Biol **225:** 229–233

Sperry JS, Holbrook NM, Zimmermann MH, Tyree MT (1987) Spring filling of xylem vessels in wild grapevine. Plant Physiol **83:** 414–417

Sun Q, Rost T, Matthews M (2008) Wound-induced vascular occlusions in *Vitis vinifera* (*Vitaceae*): tyloses in summer and gels in winter. Am J Bot **95:** 1498–1505

Tibbetts TJ, Ewers FW (2000) Root pressure and specific conductivity in temperate lianas: exotic *Celastrus orbiculatus* (*Celastraceae*) vs. native *Vitis riparia* (*Vitaceae*). Am J Bot **87:** 1272–1278

Tyree M, Salleo S, Nardini A, Mosca R, Lo Gullo M, Mosca R (1999) Refilling of embolized vessels in young stems of laurel: do we need a new paradigm? Plant Physiol **120:** 11–22

Tyree M, Sperry J (1989) Vulnerability of xylem to cavitation and embolism. Annu Rev Plant Biol **40:** 19–36

Tyree M, Zimmermann M (2002) Xylem Structure and the Ascent of Sap. Springer-Verlag, New York, pp 187–190

Tyree MT (2003) Plant hydraulics: the ascent of water. Nature **423:** 923

Utsumi Y, Sano Y, Fujikawa S, Funada R, Ohtani J (1998) Visualization of cavitated vessels in winter and refilled vessels in spring in diffuse-porous trees by cryo-scanning electron microscopy. Plant Physiol **117:** 1463–1471

Vesala T, Hölttä T, Perämäki M, Nikinmaa E (2003) Refilling of a hydraulically isolated embolized xylem vessel: model calculations. Ann Bot (Lond) **91:** 419–428

Wei C, Tyree MT, Steudle E (1999) Direct measurement of xylem pressure in leaves of intact maize plants: a test of the cohesion-tension theory taking hydraulic architecture into consideration. Plant Physiol **121:** 1191–1206

Zimmermann U, Schneider H, Wegner L, Haase A (2004) Water ascent in tall trees: does evolution of land plants rely on a highly metastable state? New Phytol **162:** 575–615

Zwieniecki M, Holbrook N (1998) Diurnal variation in xylem hydraulic conductivity in white ash (*Fraxinus americana* L.) and red spruce (*Picea rubens* Sarg.). Plant Cell Environ **21:** 1173–1180

Zwieniecki MA, Holbrook NM (2009) Confronting Maxwell's demon: biophysics of xylem embolism repair. Trends Plant Sci **14:** 530–534

Zwieniecki MA, Melcher PJ, Holbrook NM (2001a) Hydrogel control of xylem hydraulic resistance in plants. Science **291:** 1059–1062

Zwieniecki MA, Melcher PJ, Holbrook NM (2001b) Hydraulic properties of individual xylem vessels of *Fraxinus americana*. J Exp Bot **52:** 257–264